

Relativistic model for the nonmesonic weak decay of single-lambda hypernuclei

C.E. Fontoura¹, F. Krmpotić^{1,2}, A.P. Galeão¹, C. De Conti³, and G. Krein¹

¹*Instituto de Física Teórica, Universidade Estadual Paulista*

Rua Dr. Bento Teobaldo Ferraz, 271 - Bloco II, 01140-070, São Paulo, SP, Brazil

²*Instituto de Física La Plata, Universidad Nacional de La Plata, 1900 La Plata, Argentina and*

³*Campus Experimental de Rosana, Universidade Estadual Paulista, 19274-000 Rosana, SP, Brazil*

(Dated: November 11, 2021)

Having in mind its future extension for theoretical investigations related to charmed nuclei, we develop a relativistic formalism for the nonmesonic weak decay of single- Λ hypernuclei in the framework of the independent-particle shell model and with the dynamics represented by the (π, K) one-meson-exchange model. Numerical results for the one-nucleon-induced transition rates of ${}_{\Lambda}^{12}\text{C}$ are presented and compared with those obtained in the analogous nonrelativistic calculation. There is satisfactory agreement between the two approaches, and the most noteworthy difference is that the ratio Γ_n/Γ_p is appreciably higher and closer to the experimental value in the relativistic calculation. Large discrepancies between ours and previous relativistic calculations are found, for which we do not encounter any fully satisfactory explanation. The most recent experimental data is well reproduced by our results. In summary, we have achieved our purpose to develop a reliable model for the relativistic calculation of the nonmesonic weak decay of Λ -hypernuclei, which can now be extended to evaluate similar processes in charmed nuclei.

PACS numbers: 21.80.+a, 13.75.Ev, 21.60.-n

I. INTRODUCTION

Investigations of exotic nuclear properties, such as large isospin (manifest in the so called neutron-rich isotopes), or nontrivial values of flavor quantum numbers (strangeness, charm or beauty), are of continuous interest. The best known nuclei within the last category are those where a Λ -hyperon, with strangeness $S = -1$, replaces one of the nucleons, giving to the composed system some quite unusual properties. Such nuclei are referred to as Λ -hypernuclei — for recent reviews, see Refs. [1, 2].

One of the most remarkable properties of Λ -hypernuclei is the occurrence of the nonmesonic weak decay (NMWD), induced by the elementary process

$$\Lambda + N \rightarrow n + N, \quad (1)$$

with $N = p$ (proton) or n (neutron). This is the main decay channel for medium- and heavy-weight hypernuclei — Refs. [3] and [4] provide, respectively, reviews on recent theoretical and experimental developments in the study of hypernuclear decay; for earlier comprehensive reviews on theory see Refs. [5–7] and on experiment Refs. [8, 9]. NMWD can only take place within the nuclear environment and is a unique opportunity offered by nature to access the strangeness-changing interaction between baryons. Its mean lifetime has been measured in several Λ -hypernuclei and found to be of the same order of magnitude as the full mean lifetime of Λ in free space, $\tau_{\Lambda} = (2.632 \pm 0.020) \times 10^{-10}$ s [10].

The NMWD dynamics is frequently handled by one-meson-exchange (OME) models. Such models are motivated by the fact that the NN interaction at long distance is due to the one-pion-exchange, but with the difference that in NMWD the exchange processes occur with one strong and one weak vertex and can include other

mesons in addition to the π , like the pseudoscalar (K, η) and vector (ρ, ω, K^*) mesons [11–27]. The coupling constants at the strong vertices can be taken from different OME models for the NN interaction, while those at the weak vertices can be extracted from free Λ decay data and making use of soft meson theorems and $SU(6)_W$ symmetry [11, 12]. A recent study conducted within a nonrelativistic framework [25] indicates that π and K exchanges give the main contributions to the NMWD of s -shell hypernuclei.

Instead of implanting a Λ in a nucleus one could also imagine to implant a charmed baryon, like e.g. a Λ_c^+ , in view of the similarity between the quark structures of the strange and charmed hyperons, namely $\Lambda(uds)$ and $\Lambda_c^+(udc)$. Such a possibility was in fact conjectured 40 years ago [28] and several authors in the succeeding decades have found, using different models for the interactions between nucleons and charmed hyperons, that such hypothetical exotic nuclei (including even bottom nuclei) could actually form a rich spectrum of bound states over a wide range of atomic numbers [29–40]. Like Λ -hypernuclei, Λ_c^+ -hypernuclei may also decay via a NMWD process. One example is [41]

$$\Lambda_c^+ + n \rightarrow \Lambda + p, \quad (2)$$

which can be induced by the exchange of a π, ρ or K meson. Another possibility is

$$\Lambda_c^+ + N \rightarrow p + N, \quad (3)$$

induced by the exchange of a D meson. Experimentally, the literature only reports, inconclusively, the formation of three Λ_c^+ -hypernuclei, observed in a series of emulsion experiments [42, 43]. But this situation can change in a few years, with the starting of operation of the FAIR

facility in Germany and the Hadron Facility at JPARC in Japan.

There are, however, important differences between NMWD in Λ -hypernuclei and Λ_c^+ -hypernuclei. A first difference comes from the mean lifetimes of the two hyperons: $\tau_{\Lambda_c^+} \sim 10^{-3} \tau_\Lambda$. While the mean lifetime of the NMWD (1) is of the same order of magnitude of the full mean lifetime of Λ in free space, no theoretical estimate has been made for the decays (2) and (3). In addition, while the free-space decay of Λ is dominated by the pionic channels $\Lambda \rightarrow p\pi^-$ and $\Lambda \rightarrow n\pi^0$, with other decay channels contributing a thousand times less, Λ_c^+ decays in two semileptonic and numerous hadronic channels with $S = -1$ final states, having branching ratios of a few percent each. Also, decays into channels with $S = 0$ and $S = +1$ are Cabibbo-suppressed by factors of the order of 10^{-1} – 10^{-2} [10]. A second very important difference concerns the energy liberated in the decays, which is of the order of the mass difference Δ of the particles involved in the weak vertex: for the decay (2), $\Delta = M_{\Lambda_c^+} - M_\Lambda = 1170.9$ MeV, and for the decay (3), $\Delta = M_{\Lambda_c^+} - M_N = 1348.2$ MeV, which should be compared to $\Delta = M_\Lambda - M_N = 177.3$ MeV for the decay (1). One consequence of such large energy releases is that non-relativistic approaches, like those of Refs. [11–27], become inapplicable for the evaluation of NMWD transition matrix elements in charmed hypernuclei. In addition, a large energy release also implies that nuclear recoil cannot be neglected in the calculation of decay rates, particularly for light-weight nuclei. On the other hand, the interactions of the fast outgoing nucleons and/or hyperons with the residual nuclear system are expected to play a minor role.

In the present paper we develop a relativistic formalism for NMWD of hypernuclei within an independent-particle shell model (IPSM), and discuss the inclusion of recoil. Although the use of a relativistic model for the study of the structure of hypernuclei dates back to the late 1970's with Brockmann and Weise [44], so far little is known about the impact of a relativistic approach in the evaluation of NMWD rates. The first studies started 25 years ago with Ramos *et al.* [45, 46]. These authors used single-particle bound-state wave functions obtained by solving the Dirac equation with static Lorentz-scalar and -vector Woods-Saxon potentials, and transition matrix elements calculated with a (π, K) OME model. More recently, a similar approach was used by Conti *et al.* [47, 48], where the nuclear structure was described by a finite-nucleus, relativistic, mesonic-mean-field model. An interesting feature of these studies is that the reported numerical results for the decay rates differ considerably from those obtained with nonrelativistic approaches — this is true, *e.g.*, for the $^{12}_\Lambda\text{C}$ hypernucleus, as we show in Table III. Such differences are larger than one would expect given the moderate energies involved in the decay process. It is also important to notice that these predictions strongly contradict the experimental data.

Our aim in the present paper is to set up a relativis-

tic formalism for NMWD with the perspective of future applications to charmed hypernuclei. In other instances involving nuclear structure calculations at low and intermediate energies, it is often more convenient and simpler to use a relativistic approach than a nonrelativistic one [49]; this seems to be also the case for NMWD — Ref. [50] presents a very complete review on relativistic approaches for the study of nuclear structure. Although our approach for the NMWD of hypernuclei shares similarities with the formalism of Refs. [45–48], there are noteworthy differences:

1. Our final expressions for the decay rates do not involve angular momentum projection quantum numbers, since they have been summed over in closed form using the Racah algebra, which simplifies the numerical calculation;
2. Spectroscopic factors are evaluated in the second quantized formalism, as done for instance in Ref. [51], without recurring to the technique of coefficients of fractional parentage (c.f.p.'s), which is the standard antisymmetrization procedure in the first quantization framework, see *e.g.* Ref. [52];
3. We discuss the inclusion of recoil.

The predictions of our formalism are compared with available data [53–57] for the NMWD rates of the $^{12}_\Lambda\text{C}$ hypernucleus. In addition, we make a detailed comparison with results obtained in nonrelativistic approaches that include the same ingredients (like short-range correlations and OME model); such a comparison between the outcomes of analogous relativistic and nonrelativistic approaches had not been done so far.

Our formalism is explained in Section II starting from the simplest scenario, corresponding to hypernuclei with closed-shell cores and ignoring recoil, in Subsection II A. This part is done in a strictly relativistic manner, while the next two steps are performed in analogy to nonrelativistic calculations: first, in Subsection II B, we generalize the formulation to hypernuclei with open-shell cores; and secondly, in Subsection II C, the recoil effect is discussed. Subsequently, in Section III, our numerical results for the decay rates of $^{12}_\Lambda\text{C}$ are presented and compared to those of nonrelativistic calculations using a similar model [58, 59]. They are also compared with those of previous relativistic calculations and confronted with the experimental data, and a few conclusions are drawn. Finally, in Section IV, a general summary is given. In Appendices A–C, some details of the calculation are presented.

II. RELATIVISTIC DECAY RATE

To derive the NMWD rate we start from the Fermi Golden Rule. For a hypernucleus in its ground state with spin J_I and total rest energy E_I decaying into (i) two free nucleons, with asymptotic kinetic energies (T_1, T_2) , spin

projections (s_1, s_2) , and isospin projections (t_1, t_2) and (ii) the residual $(A - 2)$ -system, with spin J_F , total rest energy E_F , and kinetic energy of recoil T_R , reads

$$\Gamma_{nm} = \frac{2\pi}{(2J_I + 1)} \sum_{M_I J_F M_F} \int \frac{d\mathbf{p}_1}{(2\pi)^3} \frac{d\mathbf{p}_2}{(2\pi)^3} \delta(E_I - E_F - \mathcal{E}) \times |\overline{\mathcal{M}}(\mathbf{p}_1 \mathbf{p}_2 s_1 s_2 t_1 t_2 J_F M_F, J_I M_I)|^2, \quad (4)$$

where $\mathcal{E} = 2M_N - T_R - T_2 - T_1$, $\overline{\mathcal{M}} = (1 - P_{12})\mathcal{M}/\sqrt{2}$ is the antisymmetrized and normalized relativistic matrix element that is specified below, M_N is the nucleon mass, and $p_i = \sqrt{E_i^2 - M_N^2}$ and $E_i = T_i + M_N$ are the asymptotic momenta and total energies of the outgoing particles ($i = 1, 2$). We use unitary, as opposed to covariant, normalization for the momentum eigenspinors; for details see Section 2.2 of Ref. [60]. We average over the spin projections M_I of the initial hypernucleus and sum over the final spin projections M_F . For the nuclear structure framework, the IPSM is used, while the dynamics is described by an OME potential containing always one weak vertex W and one strong vertex S, as illustrated in Figure 1. In the IPSM it is assumed that: (i)

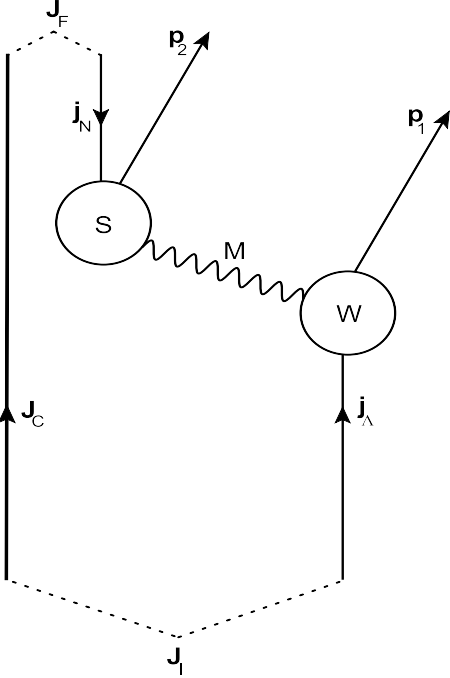


FIG. 1. Diagrammatic representation of the hypernuclear nonmesonic weak decay from the initial state $|J_I\rangle \equiv |(J_C j_\Lambda) J_I\rangle$ to the final state $|J_F\rangle \equiv |(J_C j_N^{-1}) J_F\rangle$ while two nucleons with momenta \mathbf{p}_1 and \mathbf{p}_2 are emitted into the continuum. S and W are the strong and the weak vertices, respectively, and M is a nonstrange meson. For a strange meson, the natures of the two vertices should be interchanged.

the initial hypernuclear state can be approximated as a Λ -hyperon in the single-particle state $j_\Lambda = 1s_{1/2}$ weakly

coupled to an $(A - 1)$ nuclear core of spin J_C and total rest energy E_C , *i.e.*, $|J_I\rangle \equiv |(J_C j_\Lambda) J_I\rangle$, having energy $E_I = E_C + \varepsilon_{j_\Lambda} + M_\Lambda$; (ii) the nucleon N inducing the decay is in the single-particle state j_N ($j \equiv nlj$); (iii) the final residual nuclear states have the form $|J_F\rangle \equiv |(J_C j_N^{-1}) J_F\rangle$ with energy $E_F = E_C - \varepsilon_{j_N} - M_N$; (iv) the liberated kinetic energy is

$$T_R + T_2 + T_1 = E_I - E_F - 2M_N \equiv \Delta_{j_N} = \Delta + \varepsilon_{j_\Lambda} + \varepsilon_{j_N} \quad (5)$$

where $\Delta = M_\Lambda - M_N = 177$ MeV, and the ε 's are single-particle energies.

A. Hypernuclei with doubly-closed shell cores and without recoil

Taking the simplest possible case in Eq. (4), we will start with hypernuclei whose cores contain only doubly-closed subshells, as, for instance, ${}^5_\Lambda\text{He}$, ${}^{13}_\Lambda\text{C}$, ${}^{17}_\Lambda\text{O}$, and we will omit the recoil effect. Thus, $J_C = 0$, $J_I = j_\Lambda$, $M_I = m_\Lambda$, $J_F = j_N$, $M_F = m_N$, and the transition amplitude \mathcal{M} is just the two-body T-matrix for the direct OME process. When a pseudoscalar coupling is considered for the strong vertex, one has for the pion plus kaon meson exchange: $\mathcal{M} = \mathcal{M}^\pi + \mathcal{M}^K$, see [46, Eq. (3)] and [47, Eqs.(7),(45)], with

$$\mathcal{M}^\pi(\mathbf{p}_1 \mathbf{p}_2 s_1 s_2 t_1 t_2 j_N m_N j_\Lambda m_\Lambda) = \int d\mathbf{x} d\mathbf{y} \bar{\psi}_{\mathbf{p}_1 s_1}(\mathbf{x}) [\mathcal{A}^\pi(t_1, t_2) - \mathcal{B}^\pi(t_1, t_2) \gamma_5] \times \Psi_{j_\Lambda m_\Lambda}(\mathbf{x}) \Delta^\pi(|\mathbf{x} - \mathbf{y}|) \bar{\psi}_{\mathbf{p}_2 s_2}(\mathbf{y}) \gamma_5 \Psi_{j_N m_N}(\mathbf{y}), \quad (6)$$

and

$$\mathcal{M}^K(\mathbf{p}_1 \mathbf{p}_2 s_1 s_2 t_1 t_2 j_N m_N j_\Lambda m_\Lambda) = \int d\mathbf{x} d\mathbf{y} \bar{\psi}_{\mathbf{p}_1 s_1}(\mathbf{x}) \gamma_5 \Psi_{j_\Lambda m_\Lambda}(\mathbf{x}) \Delta^K(|\mathbf{x} - \mathbf{y}|) \times \bar{\psi}_{\mathbf{p}_2 s_2}(\mathbf{y}) [\mathcal{A}^K(t_1, t_2) - \mathcal{B}^K(t_1, t_2) \gamma_5] \Psi_{j_N m_N}(\mathbf{y}), \quad (7)$$

where we are using the following definitions

$$\begin{aligned} \mathcal{A}^\pi(t_1, t_2) &= G_F m_\pi^2 g_{\pi NN} \tilde{A}^\pi(t_1, t_2), \\ \mathcal{A}^K(t_1, t_2) &= G_F m_\pi^2 g_{K\Lambda N} \tilde{A}^K(t_1, t_2), \\ \mathcal{B}^\pi(t_1, t_2) &= G_F m_\pi^2 g_{\pi NN} \tilde{B}^\pi(t_1, t_2), \\ \mathcal{B}^K(t_1, t_2) &= G_F m_\pi^2 g_{K\Lambda N} \tilde{B}^K(t_1, t_2), \end{aligned} \quad (8)$$

with $\tilde{A}^\pi(t_1, t_2) = AI$, $\tilde{A}^K(t_1, t_2) = (IA_1 + KA_0)$, $\tilde{B}^\pi(t_1, t_2) = BI$, $\tilde{B}^K(t_1, t_2) = (IB_1 + KB_0)$ and where $I = \langle t_1 | \boldsymbol{\tau}_1 | t_\Lambda = -\frac{1}{2} \rangle \cdot \langle t_2 | \boldsymbol{\tau}_2 | t_N \rangle$ and $K = \langle t_1 | 1_1 | t_\Lambda = -\frac{1}{2} \rangle \langle t_2 | 1_2 | t_N \rangle$ are, respectively, the isovector and isoscalar isospin factors. Here, $G_F m_\pi^2 = 2.21 \times 10^{-7}$, with G_F being the Fermi weak constant and m_π the pion mass, while $g_{\pi NN} = 13.3$ and $g_{K\Lambda N} = -14.1$ are the strong vertex couplings [61]. The pion parity-violating (PV) and parity-conserving (PC) weak coupling constants are adjusted to the free Λ -decay giving, respectively, $A = 1.05$ and $B = -7.15$, while the kaon weak

couplings

$$\begin{aligned} A_0 &= \frac{C_K^{PV}}{2} + D_K^{PV}, \quad A_1 = \frac{C_K^{PV}}{2}, \\ B_0 &= \frac{C_K^{PC}}{2} + D_K^{PC}, \quad B_1 = \frac{C_K^{PC}}{2}, \end{aligned} \quad (9)$$

with $C_K^{PV} = 0.76$, $C_K^{PC} = -18.9$, $D_K^{PV} = 2.09$, and $D_K^{PC} = 6.63$, have been estimated theoretically [11].

The propagator $\Delta^M(|\mathbf{x}-\mathbf{y}|)$ ($M = \pi, K$) reads [47, 48]:

1. For $(q_0)^2 < m_M^2$,

$$\begin{aligned} \Delta^M(|\mathbf{x}-\mathbf{y}|) &= -\frac{\exp(-\sqrt{m_M^2 - q_0^2}|\mathbf{x}-\mathbf{y}|)}{4\pi|\mathbf{x}-\mathbf{y}|} \\ &\quad + \Delta_F^M(\mathbf{x}-\mathbf{y}), \end{aligned} \quad (10)$$

where q_0 is the energy carried by the exchanged meson, and

$$\begin{aligned} \Delta_F^M(|\mathbf{x}-\mathbf{y}|) &= -\frac{\exp(-\sqrt{\Lambda_M^2 - q_0^2}|\mathbf{x}-\mathbf{y}|)}{4\pi|\mathbf{x}-\mathbf{y}|} \\ &\quad + \frac{\Lambda_M^2 - m_M^2}{8\pi\sqrt{\Lambda_M^2 - q_0^2}} \exp(-\sqrt{\Lambda_M^2 - q_0^2}|\mathbf{x}-\mathbf{y}|), \end{aligned} \quad (11)$$

is the finite-size correction when dipole form factors with cut-off parameters Λ_M ($M = \pi, K$) are attached at each vertex;

2. For $m_M^2 < (q_0)^2 < \Lambda_M^2$,

$$\Delta^M(|\mathbf{x}-\mathbf{y}|) = -\frac{\exp(i\sqrt{q_0^2 - m_M^2}|\mathbf{x}-\mathbf{y}|)}{4\pi|\mathbf{x}-\mathbf{y}|}. \quad (12)$$

Therefore the propagator is now complex [47, 48] and can have oscillatory behavior, with real and imaginary parts given by

$$\Re\Delta^M(|\mathbf{x}-\mathbf{y}|) = -\frac{\cos(\sqrt{q_0^2 - m_M^2}|\mathbf{x}-\mathbf{y}|)}{4\pi|\mathbf{x}-\mathbf{y}|}, \quad (13)$$

$$\Im\Delta^M(|\mathbf{x}-\mathbf{y}|) = -\frac{\sin(\sqrt{q_0^2 - m_M^2}|\mathbf{x}-\mathbf{y}|)}{4\pi|\mathbf{x}-\mathbf{y}|}, \quad (14)$$

in this region of transferred energy.

The state of each ejected nucleon, with asymptotic momentum \mathbf{p} and spin projection s , will be approximated by a Dirac plane wave, which is expanded in spherical partial-waves as follows [62, Appendix D]:

$$\psi_{\mathbf{p}s}(\mathbf{r}) = \sum_{\kappa m} \langle \hat{\mathbf{p}}s|\kappa m \rangle^* \psi_{p\kappa m}(\mathbf{r}), \quad (15)$$

$$\langle \hat{\mathbf{p}}s|\kappa m \rangle^* = 4\pi i^l \sum_{\mu} (l\mu \frac{1}{2}s|jm) Y_{l\mu}^*(\hat{\mathbf{p}}), \quad (16)$$

$$\begin{aligned} \psi_{p\kappa m}(\mathbf{r}) &= \begin{pmatrix} f_{p\kappa}(r)\Phi_{\kappa m}(\hat{\mathbf{r}}) \\ -ig_{p\kappa}(r)\Phi_{-\kappa m}(\hat{\mathbf{r}}) \end{pmatrix} \\ &\equiv \begin{pmatrix} \uparrow\psi_{p\kappa m}(\mathbf{r}) \\ -i\downarrow\psi_{p\kappa m}(\mathbf{r}) \end{pmatrix}, \end{aligned} \quad (17)$$

where the radial partial-waves are, in unitary normalization,

$$f_{p\kappa}(r) = \sqrt{\frac{E + M_N}{2E}} j_{l_\kappa}(pr) \quad (18)$$

$$g_{p\kappa}(r) = -\text{sgn}(\kappa) \sqrt{\frac{E - M_N}{2E}} j_{\bar{l}_\kappa}(pr), \quad (19)$$

with $\kappa = \pm 1, \pm 2, \dots$, $j_\kappa = |\kappa| - 1/2$,

$$l_\kappa = \begin{cases} \kappa & \text{for } \kappa > 0 \\ -\kappa - 1 & \text{for } \kappa < 0 \end{cases}, \quad (20)$$

and $\bar{l}_\kappa = l_{-\kappa}$. (To change to covariant normalization, used in Refs.[46–48], make the replacement $\sqrt{2E} \rightarrow \sqrt{2M_N}$ in Eqs. (18) and (19) and insert the factor $M_N^2/(E_1 E_2)$ in Eq.(4).) The angular part is written, in standard notation, as

$$\Phi_{\kappa m}(\hat{\mathbf{r}}) = \sum_{s\mu} (l\mu \frac{1}{2}s|jm) Y_{l\mu}(\hat{\mathbf{r}}) \chi_s, \quad (21)$$

and the expansion coefficients $\langle \hat{\mathbf{p}}s|\kappa m \rangle^*$ fulfill the following relations

$$\sum_s \int d\hat{\mathbf{p}} \langle \hat{\mathbf{p}}s|\kappa m \rangle^* \langle \hat{\mathbf{p}}s|\kappa' m' \rangle = (4\pi)^2 \delta_{\kappa\kappa'} \delta_{mm'}, \quad (22)$$

$$\begin{aligned} 2\hat{j}^2 \delta_{jj'} \sum_{sm} \int d\hat{\mathbf{p}} \langle \hat{\mathbf{p}}s|\kappa m \rangle^* \langle \hat{\mathbf{p}}s|\kappa' m' \rangle \dots = \\ (4\pi)^2 \delta_{\kappa\kappa'} \int_{-1}^1 d\cos\theta \dots, \end{aligned} \quad (23)$$

where we are using the notation $\hat{j} = \sqrt{2j+1}$. The first of these relations can be easily verified, while the second one is shown in Appendix A. The bound-state, single-particle, wave functions read

$$\begin{aligned} \Psi_{\kappa m}(\mathbf{r}) &= \frac{1}{r} \begin{pmatrix} F_\kappa(r)\Phi_{\kappa m}(\hat{\mathbf{r}}) \\ -iG_\kappa(r)(\hat{\mathbf{r}})\Phi_{-\kappa m}(\hat{\mathbf{r}}) \end{pmatrix} \\ &\equiv \begin{pmatrix} \uparrow\Psi_{\kappa m}(\mathbf{r}) \\ -i\downarrow\Psi_{\kappa m}(\mathbf{r}) \end{pmatrix}. \end{aligned} \quad (24)$$

As explained in Appendix B, they are evaluated as in Ref. [63, Eq.(16)].

To simplify the presentation of formulas in the analytical development of Eq. (4), the intermediate steps will be exhibited only for \mathcal{M}^π , which is rewritten as

$$\begin{aligned} \mathcal{M}^\pi(\mathbf{p}_1 \mathbf{p}_2 s_1 s_2 t_1 t_2 j_N m_N j_\Lambda m_\Lambda) \\ = \sum_{\substack{\kappa_1 m_1 \\ \kappa_2 m_2}} \langle \hat{\mathbf{p}}_1 s_1 |\kappa_1 m_1 \rangle \langle \hat{\mathbf{p}}_2 s_2 |\kappa_2 m_2 \rangle \\ \times \langle p_1 \kappa_1 m_1 t_1 p_2 \kappa_2 m_2 t_2 | \Delta^\pi | \kappa_\Lambda m_\Lambda \kappa_N m_N \rangle, \end{aligned} \quad (25)$$

where we are using the following compact notation

$$\begin{aligned} \langle p_1 \kappa_1 m_1 t_1 p_2 \kappa_2 m_2 t_2 | \Delta^\pi | \kappa_\Lambda m_\Lambda \kappa_N m_N \rangle \\ \equiv \int d\mathbf{x} d\mathbf{y} \bar{\psi}_{p_1 \kappa_1 m_1}(\mathbf{x}) [\mathcal{A}^\pi(t_1, t_2) - \mathcal{B}^\pi(t_1, t_2) \gamma_5] \\ \times \Psi_{j_\Lambda m_\Lambda}(\mathbf{x}) \Delta^\pi(|\mathbf{x}-\mathbf{y}|) \bar{\psi}_{p_2 \kappa_2 m_2}(\mathbf{y}) \gamma_5 \Psi_{j_N m_N}(\mathbf{y}). \end{aligned} \quad (26)$$

Introducing these expansions in Eq. (4) gives rise to auxiliary quantities such as

$$S^\pi(p_1 t_1, p_2 t_2) \equiv \sum_{\substack{m_\Lambda m_N \\ s_1 s_2}} \int d\hat{\mathbf{p}}_1 d\hat{\mathbf{p}}_2 \delta(\Delta_{j_N} - T_1 - T_2 - T_R) \\ \times |\mathcal{M}^\pi(\mathbf{p}_1 \mathbf{p}_2 s_1 s_2 t_1 t_2 j_N m_N j_\Lambda m_\Lambda)|^2, \quad (27)$$

in which we evaluate all the summations over angular momentum projection quantum numbers and angular integrations. Neglecting recoil, *i.e.*, setting $T_R = 0$, we can use (22) for both outgoing particles getting

$$S^\pi(p_1 t_1, p_2 t_2) = (4\pi)^4 \sum_{m_\Lambda m_N} \sum_{\substack{\kappa_1 m_1 \\ \kappa_2 m_2}} \delta(\Delta_{j_N} - T_1 - T_2) \\ \times |\langle p_1 \kappa_1 m_1 t_1 p_2 \kappa_2 m_2 t_2 | \Delta^\pi | \kappa_\Lambda m_\Lambda \kappa_N m_N \rangle|^2. \quad (28)$$

Now we perform the angular momentum couplings $\vec{J} =$

$\vec{j}_\Lambda + \vec{j}_N$ and $\vec{J}' = \vec{j}_1 + \vec{j}_2$. As Δ^π is rotationally invariant, it turns out that $J = J'$, which leads to

$$\langle p_1 \kappa_1 m_1 t_1 p_2 \kappa_2 m_2 t_2 | \Delta^\pi | \kappa_\Lambda m_\Lambda \kappa_N m_N \rangle \\ = \sum_{JM} \langle p_1 \kappa_1 t_1 p_2 \kappa_2 t_2 J | \Delta^\pi | \kappa_\Lambda \kappa_N J \rangle \\ \times (j_1 m_1 j_2 m_2 | JM) (j_\Lambda m_\Lambda j_N m_N | JM), \quad (29)$$

and

$$S^\pi(p_1 t_1, p_2 t_2) = (4\pi)^4 \sum_{\kappa_1 \kappa_2 J} \hat{J}^2 \delta(\Delta_{j_N} - T_1 - T_2) \\ \times |\langle p_1 \kappa_1 t_1 p_2 \kappa_2 t_2 J | \Delta^\pi | \kappa_\Lambda \kappa_N J \rangle|^2, \quad (30)$$

where the coupled matrix element of the pion propagator is explicitly given by

$$\langle p_1 \kappa_1 t_1 p_2 \kappa_2 t_2 J | \Delta^\pi | \kappa_\Lambda \kappa_N J \rangle = -i \int d\mathbf{x} d\mathbf{y} \left\{ \left[\mathcal{A}^\pi(t_1, t_2) (\uparrow \psi_{p_1 \kappa_1}^*(\mathbf{x}) \uparrow \Psi_{\kappa_\Lambda}(\mathbf{x}) - \downarrow \psi_{p_1 \kappa_1}^*(\mathbf{x}) \downarrow \Psi_{\kappa_\Lambda}^*(\mathbf{x})) \right. \right. \\ \left. \left. + \mathcal{B}^\pi(t_1, t_2) (\uparrow \psi_{p_1 \kappa_1}^*(\mathbf{x}) \downarrow \Psi_{\kappa_\Lambda}(\mathbf{x}) + \downarrow \psi_{p_1 \kappa_1}^*(\mathbf{x}) \uparrow \Psi_{\kappa_\Lambda}(\mathbf{x})) \right] \Delta^\pi(|\mathbf{x} - \mathbf{y}|) \right. \\ \left. \times (\uparrow \psi_{p_2 \kappa_2}^*(\mathbf{y}) \downarrow \Psi_{\kappa_N}(\mathbf{y}) + \downarrow \psi_{p_2 \kappa_2}^*(\mathbf{y}) \uparrow \Psi_{\kappa_N}(\mathbf{y})) \right\}_{(j_1 j_2; j_\Lambda j_N; J)}, \quad (31)$$

with the above mentioned angular momentum couplings indicated in the last index.

At this point it is convenient to perform the tensor expansion of the propagators $\Delta^\pi(|\mathbf{x} - \mathbf{y}|)$ in the way done by de-Shalit and Talmi [52, Sec. 21] for two-body interactions, *i.e.*,

$$\Delta^\pi(|\mathbf{x} - \mathbf{y}|) = \sum_L \Delta_L^\pi(x, y) [Y_L(\hat{\mathbf{x}})_L \cdot Y(\hat{\mathbf{y}})_L] \quad (32)$$

where

$$\Delta_L^\pi(x, y) = 2\pi \int \Delta^\pi(|\mathbf{x} - \mathbf{y}|) P_L(\cos \theta_{xy}) d(\cos \theta_{xy}) \quad (33)$$

and

$$\langle \kappa_1 \kappa_2 J | [Y_L(\hat{\mathbf{x}}) \cdot Y_L(\hat{\mathbf{y}})] | \kappa_\Lambda \kappa_N J \rangle = (-)^{j_2 + j_\Lambda + J} \\ \times \left\{ \begin{matrix} j_1 & j_2 & J \\ j_N & j_\Lambda & L \end{matrix} \right\} \langle \kappa_1 || Y_L || \kappa_\Lambda \rangle \langle \kappa_2 || Y_L || \kappa_N \rangle. \quad (34)$$

It is then easy to demonstrate that

$$\langle \kappa_1 p_1 t_1 \kappa_2 p_2 t_2 J | \Delta^\pi | \kappa_\Lambda \kappa_N J \rangle = \sum_L (-)^{j_2 + j_\Lambda + J} \\ \times \left\{ \begin{matrix} j_1 & j_2 & J \\ j_N & j_\Lambda & L \end{matrix} \right\} \langle \kappa_1 p_1 t_1 \kappa_2 p_2 t_2 | \Delta_L^\pi | \kappa_\Lambda \kappa_N \rangle, \quad (35)$$

where

$$\langle \kappa_1 p_1 t_1 \kappa_2 p_2 t_2 | \Delta_L^\pi | \kappa_\Lambda \kappa_N \rangle \\ = \int xy dx dy [\mathcal{B}^\pi(t_1, t_2) B_{\kappa_1 \kappa_\Lambda}^L(x p_1) \\ - i \mathcal{A}^\pi(t_1, t_2) A_{\kappa_1 \kappa_\Lambda}^L(x p_1)] \Delta_L^\pi(x, y) C_{\kappa_2 \kappa_N}^L(y p_2) \quad (36)$$

with

$$A_{\kappa \kappa_\Lambda}^L(rp) = [f_{p\kappa}(r) F_{\kappa_\Lambda}(r) - g_{p\kappa}(r) G_{\kappa_\Lambda}(r)] \\ \times \langle \kappa || Y_L || \kappa_\Lambda \rangle, \\ B_{\kappa \kappa_\Lambda}^L(rp) = [f_{p\kappa}(r) G_{\kappa_\Lambda}(r) + g_{p\kappa}(r) F_{\kappa_\Lambda}(r)] \\ \times \langle -\kappa || Y_L || \kappa_\Lambda \rangle, \\ C_{\kappa \kappa_N}^L(rp) = [f_{p\kappa}(r) G_{\kappa_N}(r) + g_{p\kappa}(r) F_{\kappa_N}(r)] \\ \times \langle -\kappa || Y_L || \kappa_N \rangle. \quad (37)$$

The reduced matrix elements

$$\langle \kappa || Y_L || \kappa' \rangle = (4\pi)^{-1/2} (-)^{j-1/2} \hat{j} \hat{j}' \hat{L} \\ \times \left(\begin{matrix} j & L & j' \\ -\frac{1}{2} & 0 & \frac{1}{2} \end{matrix} \right) \frac{1 + (-)^{l+l'+L}}{2} \quad (38)$$

and

$$\langle -\kappa || Y_L || \kappa' \rangle = (4\pi)^{-1/2} (-)^{j-1/2} \hat{j} \hat{j}' \hat{L} \\ \times \left(\begin{matrix} j & L & j' \\ -\frac{1}{2} & 0 & \frac{1}{2} \end{matrix} \right) \frac{1 + (-)^{\bar{l}+l'+L}}{2} \quad (39)$$

fulfill the symmetry relations $\langle \kappa || Y_L || \kappa' \rangle = \langle \kappa' || Y_L || \kappa \rangle$, and $\langle \kappa || Y_L || -\kappa' \rangle = \langle -\kappa || Y_L || \kappa' \rangle$.

The K meson is incorporated through the substitution $\Delta_L^\pi \rightarrow \Delta_L = \Delta_L^\pi + \Delta_L^K$ in (36), with

$$\begin{aligned} & \langle \kappa_1 p_1 t_1 \kappa_2 p_2 t_2 | \Delta_L^K | \kappa_\Lambda \kappa_N \rangle \\ &= \int xy dx dy B_{\kappa_1 \kappa_\Lambda}^L(x p_1) \Delta_L^K(x, y) \\ & \times [\mathcal{B}^K(t_1, t_2) C_{\kappa_2 \kappa_N}^L(y p_2) - i \mathcal{A}^K(t_1, t_2) D_{\kappa_2 \kappa_N}^L(y p_2)], \end{aligned} \quad (40)$$

where

$$\begin{aligned} D_{\kappa \kappa_N}^L(rp) &= [f_{p\kappa}(r) F_{\kappa_N}(r) - g_{p\kappa}(r) G_{\kappa_N}(r)] \\ & \times \langle \kappa || Y_L || \kappa_N \rangle. \end{aligned} \quad (41)$$

Clearly the above substitution must be accompanied by the replacement $\Delta^\pi \rightarrow \Delta = \Delta^\pi + \Delta^K$ in (35), giving

$$\begin{aligned} & \langle \kappa_1 p_1 t_1 \kappa_2 p_2 t_2 J | \Delta | \kappa_\Lambda \kappa_N J \rangle = \sum_L (-)^{j_2 + j_\Lambda + J} \\ & \times \left\{ \begin{matrix} j_1 & j_2 & J \\ j_N & j_\Lambda & L \end{matrix} \right\} \langle \kappa_1 p_1 t_1 \kappa_2 p_2 t_1 | \Delta_L | \kappa_\Lambda \kappa_N \rangle. \end{aligned} \quad (42)$$

Finally, from (4),

$$\begin{aligned} \Gamma_N &= \frac{8}{\pi} \sum_{\substack{j_N t_1 t_2 \\ \kappa_1 \kappa_2 J}} \frac{\hat{j}^2}{\hat{j}_\Lambda^2} \int p_1^2 dp_1 p_2^2 dp_2 \delta(\Delta_{j_N} - T_1 - T_2) \\ & \times \left| \overline{\langle \kappa_1 p_1 t_1 \kappa_2 p_2 t_2 J | \Delta | \kappa_\Lambda \kappa_N J \rangle} \right|^2, \end{aligned} \quad (43)$$

where

$$\begin{aligned} \overline{\langle \kappa_1 p_1 t_1 \kappa_2 p_2 t_2 J \rangle} &= \frac{1}{\sqrt{2}} (|\kappa_1 p_1 t_1 \kappa_2 p_2 t_2 J\rangle \\ & - (-)^{j_1 + j_2 - J} |\kappa_2 p_2 t_2 \kappa_1 p_1 t_1 J\rangle) \end{aligned} \quad (44)$$

stand for the antisymmetrized and normalized two-particle wave functions with the isospins included. The isospin factors for the direct and exchange terms of the matrix-element in Eq. (43) are listed in Table I.

TABLE I. Isospin factors the for direct (D) and exchange (E) terms of the matrix-element in Eq. (43).

	I		K	
	n	p	n	p
D	1	-1	1	1
E	1	2	1	0

It is worth noting that the matrix elements $\overline{\langle \kappa_1 p_1 t_1 \kappa_2 p_2 t_2 J | \Delta | \kappa_\Lambda \kappa_N J \rangle}$ are in general complex, as seen from Eqs. (36) and (40). However, in the usual regime of item 1 on page 4, they are always either real or purely imaginary because there is no set of quantum numbers for which parity-conserving and parity-violating contributions interfere with each other.

To exploit the delta function in (43) we make use of the relation

$$\begin{aligned} p_i^2 dp_i &= E_i \sqrt{E_i^2 - M_N^2} dE_i \\ &= (M_N + T_i) \sqrt{T_i(2M_N + T_i)} dT_i \end{aligned} \quad (45)$$

and get

$$\begin{aligned} \Gamma_N &= \frac{8}{\pi} \sum_{\substack{j_N t_1 t_2 \\ \kappa_1 \kappa_2 J}} \frac{\hat{j}^2}{\hat{j}_\Lambda^2} \int dT_1 dT_2 \delta(\Delta_{j_N} - T_1 - T_2) \\ & \times \rho(T_1, T_2) \left| \overline{\langle \kappa_1 p_1 t_1 \kappa_2 p_2 t_2 J | \Delta | \kappa_\Lambda \kappa_N J \rangle} \right|^2, \end{aligned} \quad (46)$$

where

$$\begin{aligned} \rho(T_1, T_2) &= (M_N + T_1) \sqrt{T_1(2M_N + T_1)} \\ & \times (M_N + T_2) \sqrt{T_2(2M_N + T_2)}. \end{aligned} \quad (47)$$

After integrating over T_2 we are left with the T_1 integration only,

$$\begin{aligned} \Gamma_N &= \frac{8}{\pi} \sum_{\substack{j_N t_1 t_2 \\ \kappa_1 \kappa_2 J}} \frac{\hat{j}^2}{\hat{j}_\Lambda^2} \int_0^{\Delta_{j_N}} dT_1 \rho(T_1, T_2) \\ & \times \left| \overline{\langle \kappa_1 p_1 t_1 \kappa_2 p_2 t_2 J | \Delta | \kappa_\Lambda \kappa_N J \rangle} \right|^2 \Big|_{T_2 = \Delta_{j_N} - T_1}, \end{aligned} \quad (48)$$

where

$$\begin{aligned} & \overline{\langle \kappa_1 p_1 t_1 \kappa_2 p_2 t_2 J | \Delta | \kappa_\Lambda \kappa_N J \rangle} \\ &= \frac{1}{\sqrt{2}} (\langle \kappa_1 p_1 t_1 \kappa_2 p_2 t_2 J | \Delta | \kappa_\Lambda \kappa_N J \rangle \\ & - (-)^{j_1 + j_2 - J} \langle \kappa_2 p_2 t_2 \kappa_1 p_1 t_1 J | \Delta | \kappa_\Lambda \kappa_N J \rangle). \end{aligned} \quad (49)$$

The direct matrix element is given by (42) and the exchange one is obtained through the transposition $(\kappa_1, p_1, t_1) \leftrightarrow (\kappa_2, p_2, t_2)$.

B. Hypernuclei with open-shell cores and without recoil

So far everything was done in the strict framework of relativistic physics. In what follows we will make use of analogies with nonrelativistic calculations. From previous works [21–27] done by our group, we know that to describe the hypernuclei with open-shell cores within the IPSM it is enough to do the following replacement in Eq.(48)

$$\frac{\hat{j}^2}{\hat{j}_\Lambda^2} \rightarrow F_J^{j_N} \quad (50)$$

where the spectroscopic factor is given by

$$\begin{aligned} F_J^{j_N} &= \hat{j}^{-2} \sum_{J_F} |\langle J_I || (a_{j_N}^\dagger a_{j_\Lambda}^\dagger)_J || J_F \rangle|^2 \\ &= \hat{j}^2 \sum_{J_F} \left\{ \begin{matrix} J_C & J_I & j_\Lambda \\ J & j_N & J_F \end{matrix} \right\}^2 |\langle J_C || a_{j_N}^\dagger || J_F \rangle|^2. \end{aligned} \quad (51)$$

As previously mentioned, to evaluate the spectroscopic amplitudes $\langle J_C || a_{j_N}^\dagger || J_F \rangle$, instead of employing the c.f.p.'s [52] that have been thoroughly used in, both non-relativistic [12], and relativistic [46–48] calculations, we

use the second quantization formalism. In (51) the summation goes only over the values of J_F that fulfill the constraint $|J_C - j_N| \leq J_F \leq J_C + j_N$. The values for J_I and J_C are taken from experimental data and, for most hypernuclei of interest, are listed in Table I of Ref. [23]. The resulting factors $F_J^{j_N}$ are listed in Table II of the same paper.

Therefore, when the recoil effect is not taken into account, the NMWD transition rate in open shell hypernuclei reads

$$\Gamma_N = \frac{8}{\pi} \sum_{\substack{j_N t_1 t_2 \\ \kappa_1 \kappa_2 J}} F_J^{j_N} \int_0^{\Delta_{j_N}} dT_1 \rho(T_1, T_2) \times \left| \overline{\langle \kappa_1 p_1 t_1 \kappa_2 p_2 t_2 J | \Delta | \kappa_\Lambda \kappa_N J \rangle} \right|_{T_2 = \Delta_{j_N} - T_1}^2. \quad (52)$$

We note that, while Eq. (48) is only valid for doubly-closed-shell hypernuclei, Eq. (52) is valid for both closed- and open-shell hypernuclei.

C. Inclusion of the recoil effect

As seen above, when the recoil is neglected one can perform first the full angular integration $\int d\hat{\mathbf{p}}_1 \int d\hat{\mathbf{p}}_2$, leading to a great simplification of the resulting expression. It is self-evident that this cannot be done anymore in the presence of the recoil energy

$$E_R = \sqrt{M_R^2 + p_1^2 + p_2^2 + 2p_1 p_2 \cos \theta_{12}}, \quad (53)$$

where M_R is the relativistic rest mass of the recoiling nucleus. However, once the hypernucleus is unpolarized (and unaligned), there is no preferred axis along which to orient vectors. Therefore, we can choose to orient \mathbf{p}_2 with respect to \mathbf{p}_1 and write

$$\int d\hat{\mathbf{p}}_1 \int d\hat{\mathbf{p}}_2 \cdots = \int d\hat{\mathbf{p}}_1 \int d\hat{\mathbf{p}}_{12} \cdots = \int d\phi_1 \int d\cos \theta_1 \int d\phi_{12} \int d\cos \theta_{12} \cdots. \quad (54)$$

Consequently, we can use (22) for integration on $\hat{\mathbf{p}}_1$ and (23) for integration on $\hat{\mathbf{p}}_{12}$, with the result that, as shown in Appendix C, instead of (30) we have now

$$S^\pi(p_1 t_1, p_2 t_2) = \frac{(4\pi)^2}{2} \sum_{\kappa_1 \kappa_2 J} \hat{j}^2 \int d\cos \theta_{12} \delta(\Delta_{j_N} - T_1 - T_2 - T_R) \times \left| \langle p_1 \kappa_1 t_1 p_2 \kappa_2 t_2 J | \Delta^\pi | \kappa_\Lambda \kappa_N J \rangle \right|^2. \quad (55)$$

From comparison with (30) one concludes that the results developed so far hold valid even when the recoil effect is included, as long as one makes the replacement:

$$\int p_1^2 dp_1 p_2^2 dp_2 \delta(\Delta_{j_N} - T_1 - T_2) \cdots \rightarrow \frac{1}{2} \int d\cos \theta_{12} p_1^2 dp_1 p_2^2 dp_2 \times \delta(\Delta_{j_N} - T_1 - T_2 - T_R) \cdots. \quad (56)$$

For the sake of convenience we will work here with the nonrelativistic limit for the kinetic energy of recoil, *i.e.*, with

$$T_R = E_R - M_R \cong \frac{p_1^2 + 2p_2^2 + p_1 p_2 \cos \theta_{12}}{2M_R} \cong \frac{M_N}{M_R} (T_1 + T_2 - 2\sqrt{T_1 T_2} \cos \theta_{12}) \quad (57)$$

which we consider to be good enough for the present purposes. Moreover, we neglect the binding energy of the recoiling nucleus, and take $M_R = M_N(A - 2)$. The transition rate becomes then

$$\Gamma_N = \frac{4}{\pi} \sum_{\substack{j_N t_1 t_2 \\ \kappa_1 \kappa_2 J}} F_J^{j_N} \int dT_1 dT_2 d\cos \theta_{12} \rho(T_1, T_2) \times \left| \overline{\langle \kappa_1 p_1 t_1 \kappa_2 p_2 t_2 J | \Delta | \kappa_\Lambda \kappa_N J \rangle} \right|^2 \times \delta(\Delta_{j_N} - T_R - T_1 - T_2). \quad (58)$$

To perform the integration on T_2 we introduce an auxiliary variable x , defined as $T_2 = p_2^2 / (2M_N) \equiv x^2$, *i.e.*,

$$\delta(T_2 + T_1 + T_R - \Delta_{j_N}) dT_2 = \frac{A - 2}{A - 1} \times \delta(x^2 + T_1 - \Delta_{j_N} \frac{A - 2}{A - 1} - \frac{2x \cos \theta_{12}}{A - 1} \sqrt{T_1}) 2x dx = \frac{A - 2}{A - 1} \frac{2x dx}{|x^+ - x^-|} [\delta(x - x^+) + \delta(x - x^-)], \quad (59)$$

where

$$x^\pm = \frac{\sqrt{T_1} \cos \theta_{12}}{A - 1} \pm \sqrt{\frac{T_1 \cos^2 \theta_{12}}{(A - 1)^2} + \Delta_{j_N} \frac{A - 2}{A - 1} - T_1}. \quad (60)$$

Therefore

$$\Gamma_N = \frac{8}{\pi} \frac{A - 2}{A - 1} \sum_{\substack{j_N t_1 t_2 \\ \kappa_1 \kappa_2 J}} F_J^{j_N} \times \int dT_1 d\cos \theta_{12} dx x \rho(T_1, T_2) \times \left| \overline{\langle \kappa_1 p_1 t_1 \kappa_2 p_2 t_2 J | \Delta | \kappa_\Lambda \kappa_N J \rangle} \right|^2 \times \frac{\delta(x - x^+) + \delta(x - x^-)}{|x^+ - x^-|}. \quad (61)$$

After integrating on x one gets

$$\Gamma_N = \frac{4}{\pi} \sum_{\substack{j_N t_1 t_2 \\ \kappa_1 \kappa_2 J}} F_J^{j_N} \times \int dT_1 d\cos \theta_{12} \left\{ \left[\rho'(T_1, T_2, \cos \theta_{12}, \Delta_{j_N}) \times \left| \overline{\langle \kappa_1 p_1 t_1 \kappa_2 p_2 t_2 J | \Delta | \kappa_\Lambda \kappa_N J \rangle} \right|^2 \right]_{x \rightarrow x^+} + \left[\cdot \right]_{x \rightarrow x^-} \right\}, \quad (62)$$

where

$$\rho'(T_1, T_2, \cos \theta_{12}, \Delta_{j_N}) = \frac{x(A-2)\rho(T_1, T_2)}{\sqrt{T_1 \cos^2 \theta_{12} + \Delta_{j_N}(A-2)(A-1) - T_1(A-2)^2}}. \quad (63)$$

It might be useful to mention here that:

- In the analogous nonrelativistic formulation, it has been shown numerically that the contribution corresponding to the second term in Eq. (62) is negligibly small compared to that of the first [23]. Whether this also occurs in relativistic calculations must still be verified.
- In the limit $A \rightarrow \infty$, the result (52) is recovered. Indeed, once

$$x^\pm \xrightarrow{A \rightarrow \infty} \pm \sqrt{\Delta_{j_N} - T_1},$$

x^- becomes unphysical. Therefore, the only contribution comes from the first term in (62), and, as can be seen from (63),

$$\int d \cos \theta_{12} \rho'(T_1, T_2, \cos \theta_{12}, \Delta_{j_N}) \xrightarrow{A \rightarrow \infty} 2\rho(T_1, T_2).$$

III. NUMERICAL RESULTS

We present here our results for the NMWD rates of ^{12}C . The recoil effect has been neglected since we have learned in our previous nonrelativistic calculations [21–23, 25–27] that, although it is relevant for the energy distribution of emitted particles in very light systems, such as s-shell hypernuclei, and is crucial for the angle distribution in general, it is less important for the integrated rates. Therefore Eq. (52) has been used.

Two approaches have been tested for the propagators $\Delta^M(|\mathbf{x} - \mathbf{y}|)$, both based on the fact that the ranges of Yukawa-like baryon-baryon forces within hypernuclei depend not only on the intermediate meson mass but also on the baryon masses, as stated in [64, Appendix G], namely,

RA1: This is the standard approach in nonrelativistic calculations [16, 18, 65], where the energy q_0 carried by the exchanged meson is constant and always smaller than the meson mass m_M , having the value $q_0 = \Delta/2 = 88.5$ MeV. This implies that the factor $\sqrt{m_M^2 - q_0^2}$ in (10) is taking the place of the effective mass $\tilde{m}_M = \sqrt{m_M^2 - \Delta^2/4}$.

RA2: This is the approach introduced in Refs. [47, 48], which is more appropriate for relativistic calculations, where q_0 is evaluated for each value of the kinetic energy T_1 , with direct and exchange energies being respectively $q_0^D = \Delta + \varepsilon_{j_A} - T_1$,

and $q_0^E = T_1 - \varepsilon_{j_N}$. Once for the NMWD in Λ -hypernuclei the energy transfer is of the order 50–150 MeV, q_0 can be larger than m_π and the factor $\sqrt{m_\pi^2 - q_0^2}$ can become complex. Therefore, in the case of the π meson, besides making use of Eqs. (10) and (11), one also needs Eq. (12). We are particularly interested in this approach, since, as mentioned above, the transfer of energy in the NMWD of charmed nuclei can reach much higher values.

Initial and final short range correlations (SRC) were included as in the nonrelativistic case, *i.e.*, by making the substitution

$$\Delta^M(r) \rightarrow g_f(r)\Delta^M(r)g_i(r) \quad (64)$$

in the tensor expansion (32), where $r \equiv |\mathbf{x} - \mathbf{y}|$ and

$$g_i(r) = \left(1 - e^{-r^2/\alpha^2}\right)^2 + \beta r^2 e^{-r^2/\gamma^2},$$

$$g_f(r) = 1 - j_0(q_c r) \quad (65)$$

are, respectively, the initial and final SRC, with $\alpha = 0.5$ fm, $\beta = 0.25$ fm⁻², and $\gamma = 1.28$ fm, and $q_c = 3.93$ fm⁻¹ [12, 16, 18, 46–48]. The dipole form-factor cutoffs $\Lambda_\pi = 1.3$ GeV and $\Lambda_K = 1.2$ GeV are also the same as in these works. We present here two different sorts of comparisons involving our results for the decay rates of ^{12}C . First, in Table II, the two relativistic calculations RA1 and RA2 are compared with each other, and also with the analogous nonrelativistic (NR) calculation using the RA1 approach for the propagator. The NR calculation is analogous to the relativistic ones in the sense that it uses the same OME model, the same SRC, the same single-particle energies, and single-particle wave functions of a harmonic oscillator potential with size parameter $b = 1.60$ fm, which gives the same root-mean-square radius for the initial hypernucleus. We show the decay rates Γ_n and Γ_p , the total one-nucleon-induced nonmesonic decay rates $\Gamma_{nm} = \Gamma_n + \Gamma_p$, and the ratios Γ_n/Γ_p within different OME models, namely, the π and (π, K) exchanges without and with SRC. Clearly, the relativistic calculations were evaluated in the laboratory frame of reference (LFR). Therefore, we confront them with NR calculations that also were done in the LFR. These, in turn, have been shown elsewhere [58, 59] to nicely agree with the NR evaluation within center-of-mass frame (CMF). It is not possible here to separate the decay rates Γ_n and Γ_p in the usual Block-Dalitz channels [66]

$$\begin{aligned} \mathbf{a} &\doteq {}^1\text{S}_0 \rightarrow {}^1\text{S}_0, & \mathbf{b} &\doteq {}^3\text{P}_0 \rightarrow {}^1\text{S}_0, & \mathbf{c} &\doteq {}^3\text{S}_1 \rightarrow {}^3\text{S}_1, \\ \mathbf{d} &\doteq {}^3\text{D}_1 \rightarrow {}^3\text{S}_1, & \mathbf{e} &\doteq {}^1\text{P}_1 \rightarrow {}^3\text{S}_1, & \mathbf{f} &\doteq {}^3\text{P}_1 \rightarrow {}^3\text{S}_1, \end{aligned} \quad (66)$$

as one can always do in the CMF within the s-wave approximation [24]. Therefore, we only show separate results for the parity-conserving (PC) and parity-violating (PV) parts of the decay rates, which contain, respectively, the $(\mathbf{a} + \mathbf{c} + \mathbf{d})$ and $(\mathbf{b} + \mathbf{e} + \mathbf{f})$ contributions. From Table II it can be concluded that:

TABLE II. Comparison between the nonrelativistic (NR) and relativistic results for Γ_n , Γ_p , $\Gamma_{nm} = \Gamma_n + \Gamma_p$, and Γ_n/Γ_p in ${}^{12}_\Lambda\text{C}$, for different OME models, *i.e.*, the π and $\pi + K$ exchanges without and with SRC. To allow a more detailed comparison, parity-conserving (PC) and parity-violating (PV) parts of Γ_n and Γ_p are given separately. As explained in the text, two approximations were used for the propagators in the relativistic calculations, namely RA1 and RA2. All results are in units of the free Λ decay rate $\Gamma_\Lambda = 2.50 \times 10^{-12}$ MeV.

Model	$\Gamma_n^{(\text{PC})}$	$\Gamma_n^{(\text{PV})}$	$\Gamma_p^{(\text{PC})}$	$\Gamma_p^{(\text{PV})}$	Γ_n/Γ_p	Γ_{nm}
NR						
No SRC						
π	0.1084	0.1592	0.8717	0.4017	0.2102	1.5410
$\pi + K$	0.0286	0.1851	0.3748	0.3550	0.2929	0.9434
SRC						
π	0.0122	0.1753	0.8062	0.4475	0.1495	1.4412
$\pi + K$	0.0161	0.1945	0.3822	0.3985	0.2697	0.9913
RA1						
No SRC						
π	0.1207	0.1531	0.6894	0.3309	0.2683	1.2941
$\pi + K$	0.0555	0.2394	0.3955	0.3825	0.3790	1.0729
SRC						
π	0.0969	0.1226	0.5210	0.2447	0.2866	0.9853
$\pi + K$	0.0563	0.1648	0.3503	0.2691	0.3569	0.8405
RA2						
No SRC						
π	0.1692	0.2199	0.7875	0.4550	0.3131	1.6316
$\pi + K$	0.0988	0.3104	0.4771	0.5080	0.4154	1.3943
SRC						
π	0.1454	0.1865	0.6209	0.3619	0.3377	1.3147
$\pi + K$	0.1002	0.2317	0.4361	0.3874	0.4030	1.1554

1. Although it is clear that the inclusion of relativity sensibly affects the results, there is gross agreement between analogous nonrelativistic and relativistic calculations, both without, and with SRC.
2. The SRC, while not crucial for some decay rates, can significantly reduce others, both in the nonrelativistic and in the relativistic cases.
3. The decay rates Γ_n and Γ_p are both higher in RA2 than in RA1.
4. Relativity tends to make Γ_n become larger and Γ_p smaller, and this effect is more pronounced in the RA2 approach for the propagator. As a consequence the relativistic n/p ratio becomes significantly larger than the nonrelativistic one. Therefore, the relativistic approach, specially RA2, helps to solve the longstanding puzzle on the Γ_n/Γ_p ratio [16, 67]. (See also Table III.)

Then, in Table III, are compared the present RA2 calculations for ${}^{12}_\Lambda\text{C}$ with previous relativistic calculations performed by Ramos *et al.* [46], and by Conti *et*

al. [47, 48] for several OME models. The differences between the three theoretical calculations are very large. We do not know the reason for such huge differences, although there are several possibilities. First, they could be due to the way in which the spectroscopic factors are evaluated, and how the states of the two emitted particles are antisymmetrized and normalized. Secondly, differences can arise simply from numerical errors. To avoid those, we have checked step by step the entire relativistic calculation with the nonrelativistic one.

In the same Table III are shown the pertinent experimental data produced by the KEK and FINUDA groups [53–57]. When confronted with the several relativistic theoretical results, it is easy to discover that only the present evaluation within the $\pi + K + \text{SRC}$ model agrees well with the available data. In particular, the good agreement for the ratio Γ_n/Γ_p should be highlighted. The only significant discrepancy is with the experimental values for Γ_n and Γ_p obtained by KEK in Ref. [53]. However, there is agreement with the experimental value for Γ_p obtained by FINUDA in Ref. [57]. As to the last column in Tables II and III, it is important to remark that, while all the listed calculations include only one-nucleon-induced transitions, the experimental values include also eventual two-nucleon-induced contributions.

IV. SUMMARY AND FINAL REMARKS

Starting from the Fermi Golden Rule (4) we present in Section II a relativistic formalism to describe the non-mesonic weak decay of single- Λ hypernuclei within the framework of the IPSM, with the dynamics represented by the (π, K) OME model. First, in Subsection II A we do this for hypernuclei whose cores have only closed subshells, and when the recoil effect is disregarded. Here, the Dirac plane waves are expanded in spherical partial-waves, the multipole expansion of the propagator is done, and the two-body matrix element is properly antisymmetrized with regard to the two outgoing nucleons. Making use of the orthogonality condition (22) and exploring the energy conserving δ -function, the six momentum-space integrals in Eq.(4) are reduced to one in Eq.(48), to be performed numerically. Next, the derived result is generalized to include hypernuclei with open-shell cores. This is done by means of the spectroscopic factors given by Eq.(51), which are evaluated in second quantization, without recurring to the c.f.p. technique. In this way we arrive at Eq.(52). Finally, in Subsection II C we discuss the recoil effect, which is important not only for the evaluation of angular distributions of the pairs of emitted nucleons, but also for the study of single kinetic energy spectra in light and medium-weight hypernuclei.

Numerical results for ${}^{12}_\Lambda\text{C}$ are presented in Section III. Firstly, Table II shows the comparison between analogous nonrelativistic and relativistic calculations of the transition rates Γ_n and Γ_p . The parity-conserving and parity-violating contributions are given separately. Such

TABLE III. Results for the nonmesonic decay rates Γ_n , Γ_p and $\Gamma_{nm} = \Gamma_n + \Gamma_p$, and the ratio Γ_n/Γ_p in $^{12}_\Lambda\text{C}$ for several OME models, namely, the π and $\pi + K$ exchanges without and with SRC. The present calculations with the approach RA2 for the propagators are compared with previous relativistic calculations performed by Refs. [46–48] and with the experimental data [53–57]. All results are in units of $\Gamma_0 = 2.50 \times 10^{-12}$ MeV.

Model	Γ_n	Γ_p	Γ_n/Γ_p	Γ_{nm}
<u>π</u>				
Present (RA2)	0.39	1.24	0.31	1.63
Ref. [46]	0.27	1.32	0.20	1.62
Ref. [47, 48]	0.89	2.08	0.41	2.95
<u>π+SRC</u>				
Present (RA2)	0.33	0.98	0.34	1.31
Ref. [46]	0.06	0.29	0.20	0.35
Ref. [47, 48]	1.80	0.62	0.34	2.42
<u>$\pi + K$</u>				
Present (RA2)	0.41	0.98	0.41	1.39
Ref. [47, 48]	1.24	1.59	0.78	2.84
<u>$\pi + K$+SRC</u>				
Present (RA2)	0.33	0.82	0.40	1.15
Ref. [46]	0.05	0.36	0.15	0.41
Ref. [47, 48]	0.96	1.42	0.67	2.38
<u>Experiment</u>				
Ref. [53]	0.23 ± 0.08	0.45 ± 0.10	–	–
Ref. [54]	–	–	$0.51 \pm 0.13 \pm 0.05$	–
Ref. [55]	–	–	–	$0.828 \pm 0.056 \pm 0.066$
Ref. [56]	–	–	–	0.953 ± 0.032
Ref. [57]	–	0.65 ± 0.19	–	–

a comparison is crucial so that one can rely on relativistic calculations. However, it had never been done before. The agreement is satisfactory, and the only difference worth mentioning is that the ratio Γ_n/Γ_p is appreciably higher in the relativistic calculation, agreeing better with experiment than the nonrelativistic one, specially when the RA2 approach to the propagators is used. Secondly, the present calculation is compared with two similar studies in Table III, from where it is clear that the discrepancies are very large. Although there are important differences with our formalism, we could not find any justification to explain this. Done in the same table, the comparison of our calculation with the available experimental data is encouraging and favors the $\pi + K + \text{SRC}$ OME model.

In short, we have achieved our goal of developing a reliable relativistic model for calculating the nonmesonic weak decay of Λ -hypernuclei, which can now be extended for similar weak decays in charmed nuclei. In parallel with this development, we intend to incorporate in our formalism the final state distortions of the outgoing nucleon waves induced by the interaction with the residual nucleus by making use of a relativistic optical potential.

ACKNOWLEDGMENTS

Work partially supported by the Argentinean agencies Consejo Nacional de Investigaciones Científicas y

Técnicas - CONICET, Grant No.PIP 0377 (F.K.), and Fondo para la Investigación Científica y Tecnológica - FONCYT, Grant No.PICT-2010-2680 (F.K.), as well as by the Brazilian agencies Fundação de Amparo à Pesquisa do Estado de São Paulo - FAPESP, Grants 2013/01790-5 (F.K.) and No. 2013/01907-0 (G.K.), and Conselho Nacional de Desenvolvimento Científico e Tecnológico - CNPq, Grant No.305894/2009-9 (G.K.). The work of C.E.F was supported by a post-graduate scholarship from Universidade Estadual Paulista.

Appendix A: Derivation of Eq. (23)

From the definition (16) it follows that

$$\begin{aligned}
& 2 \int \sum_{sm} d\hat{\mathbf{p}} \hat{j}^{-2} \delta_{jj'} \langle \hat{\mathbf{p}}s | \kappa m \rangle^* \langle \hat{\mathbf{p}}s | \kappa' m \rangle \dots \\
&= 2 \hat{j}^{-2} \delta_{jj'} (4\pi)^2 \int d\hat{\mathbf{p}} \sum_{sm} i^{l-l'} \sum_{\mu} (l\mu \frac{1}{2} s | jm) Y_{l\mu}^*(\hat{\mathbf{p}}) \\
&\times \sum_{\mu'} (l'\mu' \frac{1}{2} s | j'm) Y_{l'\mu'}(\hat{\mathbf{p}}) \dots \\
&= 2(4\pi)^2 \hat{l}^{-2} \delta_{jj'} \delta_{ll'} \int d\hat{\mathbf{p}} \sum_{\mu} Y_{l\mu}^*(\hat{\mathbf{p}}) Y_{l\mu}(\hat{\mathbf{p}}) \dots \quad (\text{A1})
\end{aligned}$$

Now, if we use the relation

$$4\pi \sum_{\mu} Y_{l\mu}^*(\hat{\mathbf{p}}) Y_{l\mu}(\hat{\mathbf{p}}) = \hat{l}^2, \quad (\text{A2})$$

we can solve the integral over the azimuthal angle to obtain

$$\begin{aligned} & 2 \int \sum_{sm} d\hat{\mathbf{p}} \hat{j}^{-2} \delta_{jj'} \langle \hat{\mathbf{p}}s | \kappa m \rangle^* \langle \hat{\mathbf{p}}s | \kappa' m \rangle \cdots \\ & = \delta_{\kappa\kappa'} (4\pi)^2 \int_{-1}^1 d\cos\theta \cdots \end{aligned} \quad (\text{A3})$$

Appendix B: Relativistic single-particle wave functions

The evaluation of the matrix elements of the NMWD is made in the context of the IPSM. This means that the Λ wave functions are those generated by spherically symmetric mesonic mean fields. That is, in solving the Dirac equations for the single-particle level of Λ , one must use the meson mean fields from the ^{12}C nucleus. This is similar in spirit to the works of Ramos *et al.* [45, 46], where single-particle bound-state wave functions are obtained by solving the Dirac equation with static Lorentz-scalar and -vector Woods-Saxon potentials.

The radial bound-state wave functions $F_{\kappa}(r)$ and $G_{\kappa}(r)$ in (24) and corresponding energy eigenvalues ε_{κ} for a single-particle state κ for the N or Λ are obtained by solving the following Dirac equations:

$$\begin{aligned} \left(\frac{d}{dr} + \frac{\kappa}{r} \right) F_{\kappa} + (\varepsilon_{\kappa} - V + S) G_{\kappa} &= 0, \\ \left(\frac{d}{dr} - \frac{\kappa}{r} \right) G_{\kappa} - (\varepsilon_{\kappa} - V - S) F_{\kappa} &= 0, \end{aligned} \quad (\text{B1})$$

where the scalar potential $S = S(r)$ is

$$S(r) = M + g_{\sigma} \sigma(r), \quad (\text{B2})$$

with $M = M_N$ and $g_{\sigma} = g_{\sigma}^N$ for the N , and $M = M_{\Lambda}$ and $g_{\sigma} = g_{\sigma}^{\Lambda}$ for the Λ ; the vector potential $V = V(r)$ for the nucleon is given by

$$V(r) = g_{\omega}^N \omega_0(r) + t_{\kappa} g_{\rho} \rho_0(r) + (t_{\kappa} + 1/2) e A_0(r), \quad (\text{B3})$$

with $t_{\kappa} = 1/2$ for the proton, $t_{\kappa} = -1/2$ for the neutron, and for the Λ it is given by

$$V(r) = g_{\omega}^{\Lambda} \omega_0(r). \quad (\text{B4})$$

The meson and Coulomb fields satisfy the following Klein-Gordon and Poisson equations

$$\begin{aligned} (-\nabla^2 + m_{\sigma}^2) \sigma &= -g_{\sigma}^N \rho_s^N - g_2 \sigma^2 - g_3 \sigma^3, \\ (-\nabla^2 + m_{\omega}^2) \omega_0 &= g_{\omega}^N \rho_B^N, \\ (-\nabla^2 + m_{\rho}^2) \rho_0 &= 1/2 g_{\rho} \rho_3, \\ -\nabla^2 A_0 &= e \rho_p, \end{aligned} \quad (\text{B5})$$

with the densities given by

$$\begin{aligned} \rho_s^N &= \sum_{\kappa} \frac{n_{\kappa}^N}{4\pi r^2} (|F_{\kappa}|^2 - |G_{\kappa}|^2), \\ \rho_B^N &= \sum_{\kappa} \frac{n_{\kappa}^N}{4\pi r^2} (|F_{\kappa}|^2 + |G_{\kappa}|^2), \\ \rho_3 &= \sum_{\kappa} \frac{(-)^{t_{\kappa}-1/2} n_{\kappa}^N}{4\pi r^2} (|F_{\kappa}|^2 + |G_{\kappa}|^2), \\ \rho_p &= \sum_{\kappa} \frac{(t_{\kappa} + 1/2) n_{\kappa}^N}{4\pi r^2} (|F_{\kappa}|^2 + |G_{\kappa}|^2), \end{aligned} \quad (\text{B6})$$

where n_{κ}^N are the nucleon occupancies of the state κ .

The system of equations is solved by iteration following the scheme of Ref. [63]: (i) we solve the Dirac equations for given initial ansätze for the S and V potentials; (ii) the solutions for $F(r)$ and $G(r)$ are then used to solve the Klein-Gordon and Poisson equations and construct new potentials; and (iii) we put these into the Dirac equations and cycle until convergence to a prescribed precision is attained. Note that the nonlinear terms for the σ field are put together with the scalar density ρ_s^N in the iteration procedure.

The numerical values of the meson-nucleon parameters are those of the column NL3 [68] of Table I in Ref. [69], and for the meson-lambda couplings are those from Ref. [70] (masses are given in MeV):

$$\begin{aligned} g_{\sigma}^N &= 10.2169, \quad g_{\omega}^N = 12.8675, \quad g_{\rho} = 8.9488, \\ e^2/4\pi &= 1/137, \quad g_{\sigma}^{\Lambda} = 0.464 g_{\sigma}^N, \quad g_{\omega}^{\Lambda} = 0.481 g_{\omega}^N, \\ g_2 &= -10.4307 \text{ fm}^{-1}, \quad g_3 = -28.8851, \\ m_{\sigma} &= 508.1941, \quad m_{\omega} = 782.501, \quad m_{\rho} = 763.000, \\ M_N &= 939, \quad M_{\Lambda} = 1116.06. \end{aligned} \quad (\text{B7})$$

TABLE IV. Single-particle energies for ^{12}C and $^{12}_{\Lambda}\text{C}$. (See text.) Experimental values for ^{12}C are taken from Ref. [46], and for $^{12}_{\Lambda}\text{C}$ from Ref. [71]. All values are in MeV.

	Calculated	Experiment
p 1s _{1/2}	-38.53	-34
p 1p _{3/2}	-13.52	-15.96
n 1s _{1/2}	-42.03	-37
n 1p _{3/2}	-16.65	-18.72
Λ 1s _{1/2}	-11.59	-10.79

In Table IV, we present the single-particle energies for ^{12}C and $^{12}_{\Lambda}\text{C}$. Note that these results are obtained without adjusting any parameters to fit experimental numbers. Clearly, a reasonable description of the experimental single-particle energies is achieved. Of course, a better description could be obtained by fine tuning the parameters, but for the purposes of the present paper such a refinement is not necessary.

Appendix C: Derivation of Eq. (55)

Here we demonstrate the result (55) starting from the definition (27) for $S^\pi(p_1 t_1, p_2 t_2)$, *i.e.*,

$$S^\pi(p_1 t_1, p_2 t_2) \equiv \sum_{\substack{m_\Lambda m_N \\ s_1 s_2}} \int d\hat{\mathbf{p}}_1 d\hat{\mathbf{p}}_2 \delta(\Delta_{j_N} - T_1 - T_2 - T_R) \\ \times |\mathcal{M}^\pi(\mathbf{p}_1 \mathbf{p}_2 s_1 s_2 t_1 t_2 j_N m_N j_\Lambda m_\Lambda)|^2. \quad (\text{C1})$$

Using the expansion (25) and making the change of variable $\hat{\mathbf{p}}_2 \rightarrow \hat{\mathbf{p}}_{12}$ as explained in Eq. (54), we are free to perform the $\hat{\mathbf{p}}_1$ integration according to Eq. (22), and are left with

$$S^\pi(p_1 t_1, p_2 t_2) = \\ (4\pi)^2 \sum_{\substack{m_\Lambda m_N \\ \kappa_1 m_1 s_2}} \int d\hat{\mathbf{p}}_{12} \delta(\Delta_{j_N} - T_1 - T_2 - T_R) \\ \times \left| \sum_{\kappa_2 m_2} \langle \hat{\mathbf{p}}_{12} s_2 | \kappa_2 m_2 \rangle \right. \\ \left. \times \langle p_1 \kappa_1 m_1 t_1 p_2 \kappa_2 m_2 t_2 | \Delta^\pi | \kappa_\Lambda m_\Lambda \kappa_N m_N \rangle \right|^2. \quad (\text{C2})$$

Then we do angular momentum algebra as in (29),

$$S^\pi(p_1 t_1, p_2 t_2) = \\ (4\pi)^2 \sum_{\substack{m_\Lambda m_N \\ \kappa_1 m_1 s_2}} \int d\hat{\mathbf{p}}_{12} \delta(\Delta_{j_N} - T_1 - T_2 - T_R) \\ \times \sum_{\substack{\kappa_2 m_2 \\ JM}} \langle \hat{\mathbf{p}}_{12} s_2 | \kappa_2 m_2 \rangle^* \langle p_1 \kappa_1 t_1 p_2 \kappa_2 t_2 J | \Delta^\pi | \kappa_\Lambda \kappa_N J \rangle^* \\ \times (j_1 m_1 j_2 m_2 | JM) (j_\Lambda m_\Lambda j_N m_N | JM) \\ \times \sum_{\substack{\kappa'_2 m'_2 \\ J' M'}} \langle \hat{\mathbf{p}}_{12} s_2 | \kappa'_2 m'_2 \rangle \langle p_1 \kappa_1 t_1 p_2 \kappa'_2 t_2 J' | \Delta^\pi | \kappa_\Lambda \kappa_N J' \rangle \\ \times (j_1 m_1 j'_2 m'_2 | J' M') (j_\Lambda m_\Lambda j_N m_N | J' M'), \quad (\text{C3})$$

to obtain

$$S^\pi(p_1 t_1, p_2 t_2) = \\ (4\pi)^2 \sum_{s_2} \int d\hat{\mathbf{p}}_{12} \delta(\Delta_{j_N} - T_1 - T_2 - T_R) \\ \times \sum_{\substack{\kappa_2 m_2 \\ \kappa'_2 m'_2}} \langle \hat{\mathbf{p}}_{12} s_2 | \kappa_2 m_2 \rangle^* \langle \hat{\mathbf{p}}_{12} s_2 | \kappa'_2 m'_2 \rangle \\ \times \sum_{\substack{\kappa_1 J \\ m_1 M}} (j_1 m_1 j_2 m_2 | JM) (j_1 m_1 j'_2 m'_2 | JM) \\ \times \langle p_1 \kappa_1 t_1 p_2 \kappa_2 t_2 J | \Delta^\pi | \kappa_\Lambda \kappa_N J \rangle^* \\ \times \langle p_1 \kappa_1 t_1 p_2 \kappa'_2 t_2 J | \Delta^\pi | \kappa_\Lambda \kappa_N J \rangle. \quad (\text{C4})$$

Due to the relation

$$\sum_{m_1 M} (j_1 m_1 j_2 m_2 | JM) (j_1 m_1 j'_2 m'_2 | JM) = \\ \frac{j_2^2}{j_2'^2} \delta_{m_2 m'_2} \delta_{j_2 j_2'}, \quad (\text{C5})$$

this reduces to

$$S^\pi(p_1 t_1, p_2 t_2) = \\ (4\pi)^2 \sum_{\substack{\kappa_2 m_2 \\ \kappa'_2 s_2}} \frac{\delta_{j_2 j_2'}}{j_2'^2} \int d\hat{\mathbf{p}}_{12} \delta(\Delta_{j_N} - T_1 - T_2 - T_R) \\ \times \langle \hat{\mathbf{p}}_{12} s_2 | \kappa_2 m_2 \rangle^* \langle \hat{\mathbf{p}}_{12} s_2 | \kappa'_2 m_2 \rangle \\ \times \sum_{\kappa_1 J} \hat{j}_2^2 \langle p_1 \kappa_1 t_1 p_2 \kappa_2 t_2 J | \Delta^\pi | \kappa_\Lambda \kappa_N J \rangle^* \\ \times \langle p_1 \kappa_1 t_1 p_2 \kappa'_2 t_2 J | \Delta^\pi | \kappa_\Lambda \kappa_N J \rangle. \quad (\text{C6})$$

Finally, using (23) one gets (55).

-
- [1] E. Botta, T. Bressani, and G. Garbarino, *Eur. Phys. J. A* **48**, 41 (2012).
[2] A. Feliciello, *Few Body Syst.* **55**, 605 (2014).
[3] G. Garbarino, *Nucl. Phys. A* **914**, 170 (2013).
[4] S. Bufalino, *Nucl. Phys. A* **914**, 160 (2013).
[5] E. Oset and A. Ramos, *Prog. Part. Nucl. Phys.* **41**, 191 (1998).
[6] W. M. Alberico and G. Garbarino, *Phys. Rep.* **369**, 1 (2002) 1.
[7] A. Parreño, *Lec. Notes Phys.* **724**, 141 (2007).
[8] H. Outa, in: *Hadron Physics*, IOS Press, Amsterdam, 2005, p. 219.
[9] J. Pochodzalla, *Acta Phys. Pol. B* **42**, 833 (2011).
[10] K.A. Olive et al. (Particle Data Group), *Chin. Phys. C* **38**, 090001 (2014).
[11] J. F. Dubach, G. B. Feldman, B. R. Holstein and L. de la Torre, *Ann. Phys. (N.Y.)* **249**, 146 (1996).
[12] A. Parreño, A. Ramos, and C. Bennhold, *Phys. Rev. C* **56**, 339 (1997).
[13] K. Itonaga, T. Ueda, and T. Motoba, *Phys. Rev. C* **65**, 034617 (2002).
[14] K. Itonaga, T. Motoba, and T. Ueda, *Mod. Phys. Lett. A* **18**, 135 (2003).
[15] K. Itonaga, T. Motoba, T. Ueda, and Th.A. Rijken, *Phys. Rev. C* **77**, 044605 (2008).
[16] C. Barbero, D. Horvat, F. Krmpotić, T. T. S. Kuo, Z. Narančić, and D. Tadić, *Phys. Rev. C* **66**, 055209 (2002).
[17] F. Krmpotić and D. Tadić, *Braz. J. Phys.* **33**, 187 (2003).
[18] C. Barbero, C. De Conti, A. P. Galeão, and F. Krmpotić, *Nucl. Phys. A* **726**, 267 (2003).

- [19] C. Barbero, A. P. Galeão, and F. Krmpotić, Phys. Rev. C **72**, 035210 (2005).
- [20] C. Barbero, A. P. Galeão, and F. Krmpotić, Phys. Rev. C **76**, 054321 (2007).
- [21] C. Barbero, A. P. Galeão, M. S. Hussein, and F. Krmpotić, Phys. Rev. C **78**, 044312 (2008)
- [22] E. Bauer, A. P. Galeão, M. S. Hussein, and F. Krmpotić, Nucl. Phys. A **834**, 599c (2010).
- [23] F. Krmpotić, A. P. Galeão, and M.S. Hussein, AIP Conf. Proc. **1245**, 51 (2010).
- [24] F. Krmpotić, Phys. Rev. C **82**, 05520 (2010).
- [25] F. Krmpotić, Few Body Syst. **55**, 219 (2014).
- [26] F. Krmpotić and C. De Conti, Int. J. of Mod. Phys. E **23**, 1450089 (2014).
- [27] I. Gonzalez, C. Barbero, A. Deppman, S. Duarte, F. Krmpotić, and O. Rodriguez, J. Phys. G: Nucl. Part. Phys. **38**, 115105 (2011).
- [28] A. A. Tyapkin, Yad. Fiz. **22**, 181 (1975).
- [29] S. Iwao, Lett. Nuovo Cim. **19**, 647 (1977).
- [30] C.B. Dover and S.H. Kahana, Phys. Rev. Lett. **39**, 1506 (1977).
- [31] R. Gatto and F. Paccanoni, Nuovo Cim. A **46**, 313 (1978).
- [32] N. N. Kolesnikov, D. I. Zhukovitsky, V. A. Kopylov, and V. I. Tarasov, Sov. J. Nucl. Phys. **34**, 533 (1981) [Yad. Fiz. **34**, 957 (1981)].
- [33] G. Bhamathi, Phys. Rev. C **24**, 1816 (1981).
- [34] H. Bando and M. Bando, Phys. Lett. B **109**, 164 (1982).
- [35] B. F. Gibson, C. B. Dover, G. Bhamathi, and D. R. Lehman, Phys. Rev. C **27**, 2085 (1983).
- [36] N. I. Starkov and V. A. Tsarev, Nucl. Phys. A **450**, 507 (1986).
- [37] C. H. Cai, L. Li, Y. H. Tan, P. Z. Ning, Europhys. Lett. **64**, 448 (2003).
- [38] K. Tsushima and F. C. Khanna, Phys. Lett. B **552**, 138 (2003).
- [39] K. Tsushima and F. C. Khanna, Phys. Rev. C **67**, 015211 (2003).
- [40] K. Tsushima and F. C. Khanna, J. Phys. G **30**, 1765 (2004).
- [41] S. A. Bunyatov, V. V. Lyukov, N. I. Starkov, and V. A. Tsarev, Sov. J. Part. Nucl. **23**, 253 (1992).
- [42] Yu. Batusov, S. A. Bunyatov, V. V. Lyukov, V. M. Sidorov, A. A. Tyapkin, and V. A. Yarba, JETP Lett. **33**, 56 (1981) [Pis'ma Zh. Eksp. Teor. Fiz. **33**, 56 (1981)].
- [43] V. V. Lyukov, Nuovo Cim. A **102**, 583 (1989).
- [44] R. Brockmann and W. Weise, Phys. Lett. B **69**, 167 (1977).
- [45] A. Ramos, C. Bennhold, E. van Meijgaard, and B.K. Jennings, Phys. Lett. B **264**, 233 (1991).
- [46] A. Ramos, E. van Meijgaard, C. Bennhold, and B.K. Jennings, Nucl. Phys. A **544**, 703 (1992).
- [47] F. Conti, "A relativistic model for the non-mesonic weak decay of the ^{12}C hypernucleus", PhD Thesis, University of Pavia, Italy, November 2009.
- [48] F. Conti, A. Meucci, C. Giusti and F. D. Pacati, arXiv:0912.3630 [nucl-th].
- [49] P. Ring, private communication.
- [50] K. Hagino and J. M. Yao, in "Relativistic Density Functional for Nuclear Structure" (World Scientific, Singapore, 2015).
- [51] R. Almar, O. Civitarese, F. Krmpotić, and J. Navaza, Phys. Rev. C **6**, 187 (1972); J. Navaza, "Descripción de Núcleos Vibracionales con el Modelo Unificado mediante Técnicas Diagramáticas", University of La Plata, Argentina, 1972.
- [52] A. de-Shalit and I. Talmi, *Nuclear Shell Theory* (Academic Press, New York, 1963).
- [53] M. Kim, *et al.*, Phys. Rev. Lett. **103**, 182502 (2009).
- [54] M. J. Kim *et al.*, Phys. Lett. B **641**, 28 (2006).
- [55] Y. Sato *et al.*, Phys. Rev. C **71**, 025203 (2005).
- [56] S. Okada *et al.*, Nucl. Phys. A **754**, 178c (2005).
- [57] M. Agnello *et al.*, Phys. Lett. B **738**, 499 (2014).
- [58] A.P. Galeão, C. Barbero, C. De Conti, and F. Krmpotić, AIP Conf. Proc. **1529**, 247 (2013).
- [59] C. De Conti, C. Barbero, A. P. Galeão, and F. Krmpotić, AIP Conf. Proc. **1625**, 181 (2014).
- [60] B. D. Serot and J. D. Walecka, Adv. Nucl. Phys. **16**, 1 (1986).
- [61] P.M.M. Maessen, Th.A. Rijken, and J.J. de Swart, Phys. Rev. C **40**, 226 (1989).
- [62] M. Doi, T. Kotani, and E. Takasugi, Prog. Theor. Phys. Supplement **83**, 1 (1985).
- [63] C.J. Horowitz and B.D. Serot, Nucl. Phys. A **368**, 503 (1981).
- [64] C. Barbero, D. Horvat, F. Krmpotić, Z. Narančić, and D. Tadić, Fizika **B 10**, 1 (2001).
- [65] K. Sasaki, M. Izaki, and M. Oka, Phys. Rev. C **71**, 035502 (2005).
- [66] M.M. Block and R.H. Dalitz, Phys. Rev. Lett. **11**, 96 (1963).
- [67] G. Garbarino, A. Parreño, and A. Ramos, Phys. Rev. Lett. **91**, (2003) 112501; Phys. Rev. C **69**, 054603 (2004).
- [68] G. A. Lalazissis, J. König, and P. Ring, Phys. Rev. C **55**, 540 (1997).
- [69] Wenjui Long, Jie Meng, N. van Giai, and S.-G. Zhou, Phys. Rev. C **69**, 034319 (2004).
- [70] M. Rufa, J. Schaffner, J. Maruhn, H. Stöcker, W. Greiner, and P.G. Reinhard, Phys. Rev. C **42**, 2469 (1990).
- [71] R.E. Chrien *et al.*, Phys. Lett. B **89**, 31 (1979).